Nonlinear Tensile Creep of Linear Low Density Polyethylene/Fumed Silica Nanocomposites: Time-Strain Superposition and Creep Prediction

Andrea Dorigato,[1] Alessandro Pegoretti,[1] Jan Kolařík[2]
[1]*Department of Materials Engineering and Industrial Technologies, University of Trento, Trento 38123, Italy*

[2]*Institute of Macromolecular Chemistry, Academy of Sciences of the Czech Republic, Prague 6 162 06, Czech Republic*

The main objectives of the study were (i) to quantitatively describe the nonlinear viscoelastic creep of model nanocomposites, (ii) to construct the generalized compliance curve by means of the tensile compliance vs. internal time superposition for a pseudo iso-free-volume state, and (iii) to predict the compliance vs. real time curves for selected stresses. To this end, the free volume theory of nonlinear viscoelastic creep developed for thermoplastics and their blend was successfully employed. Linear low density polyethylene/fumed silica nanocomposites, showing notable enhancement of the creep resistance in proportion to the surface area of incorporated nanofillers, were taken as simple model materials. POLYM. COMPOS., 31:1947–1955, 2010. © 2010 Society of Plastics Engineers

INTRODUCTION

In the recent years, rising interest has emerged in the use of inorganic nanofillers, such as silica, titania, alumina, and zirconia, to increase the rigidity, dimensional stability, and toughness of various polymeric matrices [1]. Thermoplastic materials find many applications where they are expected to sustain long lasting constant loads without excessive deformations. Thus, in many cases, poor creep resistance represents a serious deficiency [2, 3] of thermoplastics. It has been demonstrated that their reinforcement with relatively small amounts of nanofillers can be an effective solution leading to the enhancement of the creep resistance [4]. For example, titania nanoparticles markedly reduce the creep compliance of nylon 66 [5–7], while alumina nanoparticles effectively reduce the compliance of polystyrene [8]. The creep compliance of high-density polyethylene (HDPE) blown films can be significantly reduced [9] by the incorporation of maleated polyethylene and Cloisite 15A clay. A marked reduction of the creep compliance of HDPE can also be achieved by using submicrometer titania particles [10, 11] or organoclays [12]. Analogous results were reported for the viscoelastic properties of the polyimide/silica nanocomposites [13]. It is generally believed that nanoparticles can effectively restrict the mobility of polymer chains and influence the stress transfer at the nanoscale, which have positive effects on the creep resistance (dimensional stability) of the material.

Although a number of methods have been elaborated for the evaluation of the stress transfer at the fiber/matrix interfaces in microcomposites [14], no reliable method is currently available for nanocomposites. Among nanofillers that can be introduced into polymer matrices, the polymer/clay systems have mostly been studied, while less attention has been paid to the nanocomposites with fumed silica. This kind of nanoparticles is prepared by flame hydrolysis technique [15], in which a vapor precursor (such as silicon tetrachloride) is burned in hydrogen/oxygen mixture to produce the metal oxide. A series of linear low density polyethylene/fumed silica nanocomposites recently prepared by simple melt compounding has shown interesting enhancements of the stiffness, yield stress, and strain at break [16].

Quantitative analysis of the nonlinear creep, its extrapolation and/or prediction rank among very interesting fields of the materials research [17, 18]. Experimental creep data can often be fitted by a suitable equation, which facilitates their storage and processing. However, proposed equations are mainly empirical and their validity may be limited to particular materials and/or test conditions. Theoretical background of the idealized creep behavior has been well elaborated in the field of the linear viscoelasticity [19–26]. Such behavior is expected for

Correspondence to: A. Dorigato; e-mail: andrea.dorigato@ing.unitn.it
Contract grant sponsor: J.K. Grant Agency of the Czech Republic; contract grant number: 106/09/1348.
DOI 10.1002/pc.20993
Published online in Wiley Online Library (wileyonlinelibrary.com).

homogeneous and rheologically simple materials at infinitesimal deformations. However, polymeric materials used in practice are usually heterogeneous and rheologically complex and produced deformations are far from being infinitesimal [2]. For relatively high deformations, isothermal compliance (or modulus) becomes a function of both time and stress (or strain). For this reason, nonlinear viscoelastic behavior dominates over a major portion of the entire response interval of most polymeric materials and plays the key role in most applications. As the quantitative data analysis in the nonlinear creep region is much more difficult than in the linear region, a deeper understanding of the underlying processes controlling the mechanical response is required [2, 22, 23, 26–31].

Recently, the concept of a "material clock" has been introduced to describe how the retardation (or relaxation) times are controlled by the current state of the material in the course of a solicitation. According to this approach, the internal time of a material differs from the experimental (laboratory) time. Subsequently, a shift factor is introduced to convert the experimental time into the internal time in a hypothetical reference state of the material. The proposed quantities controlling a material clock are free volume [3, 28–30, 32–34], strain [30], or stress [35]. The most suitable parameter seems to be the free volume because the phenomenological theory of viscoelasticity [19–26] has shown that retardation (or relaxation) times are controlled by the fractional free volume available for molecular motions in polymeric materials. As the strain-induced increase in the specific volume can be identified with the increase in the fractional free volume [36–38], the molecular mobility in polymers is necessarily affected by tensile strains. The formulae for the shift factors have been derived, which allow us to construct a generalized creep curve over a long time interval by using the time-tensile strain superposition. The free volume approach to the nonlinear tensile creep has successfully been applied to polypropylene (PP) [18, 39], PP/styrene-acrylonitrile copolymer (SAN) [3] and PP/cycloolefin copolymer (COC) [40], and PE/COC blends [41].

This article is concerned with the nonlinear tensile creep of the LLDPE/fumed silica nanocomposites prepared via melt compounding. Our objectives are (i) to evaluate the effects of the filler and of its surface area on the nonlinear tensile creep behavior, (ii) to quantitatively describe the nonlinear creep by introducing a set of material parameters, (iii) to employ the creep data for various stresses to construct the generalized compliance curves by means of the internal time–tensile strain superposition for a pseudo iso-free-volume state, (iv) to predict the compliance–real time curves for any selected stress (lower than the yield stress).

THEORETICAL BACKGROUND

As far as the strain-induced volume increment of a polymer matrix can be identified with the increment in the free volume [36–38], increasing strain in the tensile creep produces an increase in molecular mobility and a perceptible shortening of retardation times. However, the quantitative application of this concept can be quite complex, because "auxiliary" parameters related to the polymer physical properties need to be introduced.

Empirical Function for Fitting the Creep of Polyethylene

The strain in tensile creep, $\varepsilon(t, \sigma, T)$, depending on time t, stress σ, and temperature T, is composed of three parts [21–26, 42]: (i) elastic (instantaneous, reversible) $\varepsilon_e(\sigma, T)$; (ii) viscoelastic (time-dependent, reversible) $\varepsilon_v(t, \sigma, T)$; (iii) plastic (irreversible) $\varepsilon_p(t, \sigma, T)$:

$$\varepsilon(t,\sigma,T) = \varepsilon_e(\sigma,T) + \varepsilon_v(t,\sigma,T) + \varepsilon_p(t,\sigma,T) \qquad (1)$$

If no plastic deformation is produced in the course of creeping, the tensile compliance $D(t, \sigma) = \varepsilon(t, \sigma)/\sigma$ for the isothermal nonlinear creep can be expressed as follows:

$$D(t,\sigma) = D_e(\sigma) + D_v(t,\sigma) \qquad (2)$$

In some cases, the creep compliance was tentatively expressed as a product of independent functions of time, stress, and temperature, i.e. $D(t, \sigma, T) = g_1(t)\cdot g_2(\sigma)\cdot g_3(T)$ [23, 43]. However, experimental results often indicate interrelations between these presumably independent functions. Various empirical equations were proposed to fit $D(t, \sigma)$ or $D_v(t, \sigma)$ [18, 42–44]. A relatively simple equation was found suitable for describing isothermal creep of polypropylene and of its blends [3, 18, 40, 45]:

$$\log D(t,\sigma) = \log W(\sigma) + n \log\left(\frac{t}{\tau_{rm}}\right) \qquad (3)$$

where $W(\sigma)$ is a function of stress, τ_{rm} is the mean retardation time and $0 \leq n \leq 1$ is the shape parameter reflecting the distribution of retardation times.

Tensile Creep as a Non-iso-free Volume Process

The free volume concept was widely utilized to provide satisfactory explanation for the effects of temperature, hydrostatic pressure, tensile deformation, chain ends, diluents (plasticizers), the state of physical aging, etc. on the viscoelastic behavior of polymers. The fractional free volume [19, 20, 23–26] can be defined as:

$$f = \frac{(V - V_h)}{V} = \frac{V_f}{V} \qquad (4)$$

where V is the specific volume, V_h is the specific volume occupied by molecules [25], and V_f is the free volume. The free volume is presumed [19, 38] to consist of vacancies of about the same size as mobile molecular segments. The glassy state of polymers is generally viewed [19, 20, 23–26] as an iso-free-volume state with $f_g = 0.025$. If solely the effects of temperature T and of time-dependent tensile strain $\varepsilon(t)$ are considered, the fractional free volume can be expressed as:

 DOI 10.1002/pc

$$f[T, \varepsilon(t)] = f_g + \alpha_{fv}(T - T_g) + (1 - 2v)\varepsilon(t) = f_g + \Delta f_T + \Delta f_\varepsilon \quad (5)$$

where α_{fv} is the expansion coefficient of the free volume at $T > T_g$ (which can be approximated as the difference between the expansion coefficients of the material above and below T_g, i.e., $\alpha_{fv} = \alpha_l - \alpha_g$), v is Poisson's ratio, and $[(1 - 2v)\ \varepsilon(t)]$ is the strain-induced dilatation for an isotropic material. The fractional free volume f is assumed to control retardation times τ_r in conformity with the following equation [19, 24, 46]:

$$\ln \tau_r = \ln \Omega + \frac{B}{f} \quad (6)$$

where Ω is the frequency of the thermal motion inside a potential well and B is a numerical factor related to the ratio of the volume of a jumping segment to the volume of the critical vacancy necessary for the implementation of a segment jump. The effect of f on τ_r is routinely expressed by means of the shift factor ($\log a$) along the time scale [18, 24, 28]:

$$\log a = \log \tau_r(f_2) - \log \tau_r(f_1) \quad (7)$$

where $f_2 > f_1$. The time-strain shift factor, $\log a_\varepsilon(t)$, defined as the ratio of the mean retardation time $\tau_{rm}[\varepsilon(t), T_c]$ at a strain $\varepsilon(t)$ and $\tau_{rmi}[\varepsilon_i = 0, T_c]$ for initial time $t_i = 0$ (at a constant temperature T_c) can be obtained [18] by combining *Eqs. 5* and *7*:

$$\log a_\varepsilon(t) = -\left(\frac{B}{2.303}\right) \frac{[(1 - 2v)M\varepsilon(t)/(f_g + \Delta f_{T_c})]}{[(1 - 2v)M\varepsilon(t) + (f_g + \Delta f_{Tc})]} \quad (8)$$

where M is the ratio of the average strain of the creeping phase (or component) in the multiphase test specimen and of the measured strain. Under these conditions, $\log a_\varepsilon(t)$ is not a constant for an isostress creep curve, but grows with the creep strain due to increasing free volume in the creeping specimen. If τ_{rm} of *Eq. 3* obeys *Eq. 7*, then isothermal $D(t, \sigma)$ can be expressed as:

$$\log D(t, \sigma) = [\log W(\sigma) - n \log \tau_{rmi} - n \log a_\varepsilon(t)] + n \log(t) = \log C(t, \sigma) + n \log(t) \quad (9)$$

To separate the effects of stress and time, *Eq. 9* can be rewritten in the following form:

$$\log D(t, \sigma) = [\log W(\sigma) - n \log \tau_{rmi}] + n[\log(t) - \log a_\varepsilon(t)] = \log C^*(\sigma) + n^* \log(t^*) \quad (10)$$

where parameters C^* and n^* are related to internal time t^* which reads:

$$\log t^* = \log t + \log a_\varepsilon(t) = \log t + \left(\frac{B}{2.303}\right) \frac{[(1 - 2v)M\varepsilon(t)/(f_g + \Delta f_{T_c})]}{[(1 - 2v)M\varepsilon(t) + (f_g + \Delta f_{Tc})]} \quad (11)$$

The $\log D(t)$ vs. $\log t$ plot would coincide with the $\log D(t^*)$ vs. $\log t^*$ plot for extremely low stresses and strains, for which $\Delta f_\varepsilon \to 0$; thus C^* and n^* are the limiting values of C and n for the creep in a (hypothetical) pseudo iso-free volume state.

Strain Magnification Factor for the Amorphous Phase in Crystalline Polymers

As the crystalline phase has distinctly lower compliance than the amorphous phase at $T > T_g$, the viscoelastic creep processes in semicrystalline polymers at $T > T_g$ take mainly place in the amorphous phase. To this end, semicrystalline polymer structure can be visualized in a simplified manner by a two-parameter equivalent box model (EBM) (Fig. 1), which was successfully used in the predictive formats for the moduli, yield strength, permeability, etc. [47–50] of two-component heterogeneous materials. To account for differing strains of amorphous (subscript 1) and crystalline (subscript 2) phases in the EBM, the strain-magnifying factor M can be introduced corresponding to the ratio of the average strain of the creeping phase (or component) in the multiphase test specimen and of measured strain. If a crystalline polymer is deformed, the strains of the amorphous and crystalline fractions coupled in parallel, i.e., v_{1p} and v_{2p}, are identical with the measured strain. As the crystalline phase has the compliance by two to three orders of magnitude lower than the amorphous phase above its T_g, the crystalline fraction v_{2s} (Fig. 1) coupled in series will not be perceptibly deformed during the creep process. As the displacement in the fraction v_{1s} is equal to the macroscopic displacement, the resulting strain of the amorphous phase coupled in series is higher than the measured strain; con-

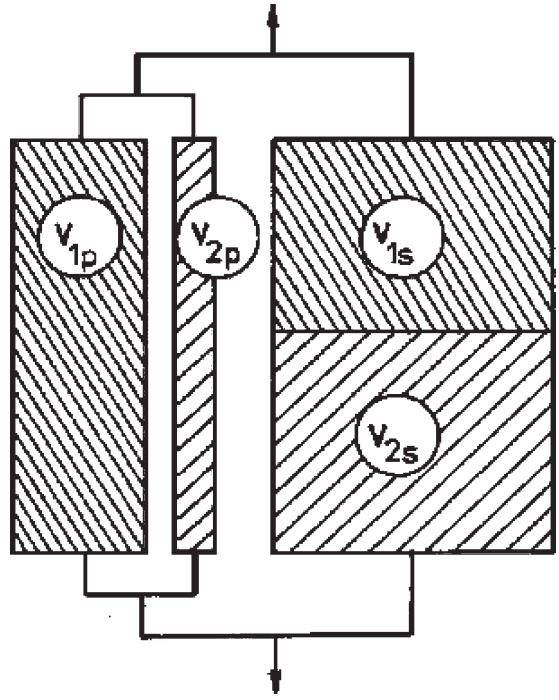

FIG. 1. Equivalent Box Model (EBM) for a two-component system (schematically).

sequently, the generation of the strain-induced free volume in the fraction v_{1s} will be higher than in the fraction v_{1p}. It was shown that the mean value of M for the amorphous phase is [3, 18, 40]:

$$M = 1 + \left(\frac{v_{2s}}{v_1}\right) \tag{12}$$

Utilizing a universal formula proposed by the percolation theory [51–53] for heterogeneous binary systems, the following equations have been derived [47–50] to determine the volume fractions of the EBM:

$$v_{1p} = \left[\frac{v_1 - v_{1cr}}{1 - v_{1cr}}\right]^q \tag{13a}$$

$$v_{2p} = \left[\frac{v_2 - v_{2cr}}{1 - v_{2cr}}\right]^q \tag{13b}$$

where v_{1cr} or v_{2cr} is the critical volume fraction (the percolation threshold) at which the phase (or component) 1 or 2 becomes partially continuous and q is the critical exponent. For three-dimensional cubic lattice, the percolation threshold $v_{cr} = 0.156$ was calculated [52, 53]. Remaining volume fractions v_{1s} and v_{2s} are evaluated by using *Eq. 14*.

$$v_{1s} = v_1 - v_{1p} \tag{14a}$$

$$v_{2s} = v_2 - v_{2p} \tag{14b}$$

Values of q were mostly reported [47, 48, 52, 53] in an interval of 1.6–2.0 so that $q = 1.8$ may be used as a typical value.

EXPERIMENTAL PART

Materials and Preparation of the Samples

Linear low density polyethylene Flexirene® CL10 was kindly supplied by Polimeri Europa (Mantova, Italy): melt flow index (MFI) at 190°C, 2.16 kg equal to 2.6 g/10′, mean numeric molecular weight of 27,000, density equal to 0.918 g/cm^3, melting point of 121°C. Flexirene® CL10 is a butene copolymer linear low density polyethylene (C_4-LLDPE) suitable for the extrusion of thin films. Two different kinds of Aerosil® fumed silica were kindly supplied by Degussa (Hanau, Germany). These nanofillers differ in the surface area, i.e. 200 m^2/g for Aerosil 200, 380 m^2/g for Aerosil 380. LLDPE chips and fumed silicas were utilized as received.

A melt compounding process followed by hot pressing was adopted for sample preparation. Thermo Haake® internal mixer was used for the compounding at 170°C for 15 min and 90 rpm. The obtained composites were then hot pressed in a Carver® press at 170°C for 15 min at low pressure (0.2 kPa), to produce 20 cm × 20 cm sheets about 0.8 mm thick. In this way the LLDPE/fumed silica nanocomposites were prepared with a constant volume loading of 2% (samples LLDPE-A200-2 and LLDPE-A380-2).

Morphological Analysis

To visualize the dispersion degree and the dimensions of fumed silica aggregates, Transmission Electron Microscopy (TEM) technique was utilized. LLDPE/A380-2 sample was observed through a Philips®/FEI CM120 transmission electron microscope, at an acceleration voltage of 80 kV. A thin section of this sample was ultramicrotomed at a temperature of about −70°C by using a Reichert-Jung® Ultracut FC4E cryo-ultramicrotome.

Tensile Creep Measurements

Creep tests of LLDPE and nanocomposites were performed at 30°C by using an Instron® 4502 tensile testing machine. Rectangular test specimens 100 mm long, 5 mm wide, and 0.8 mm thick were adopted, setting a gage length of 60 mm. As the yield strength (σ_y) of neat LLDPE was about 10 MPa, several stress levels, ranging from 1 to 5 MPa, were applied in creep experiments. The total time of the creep tests was 1200 s. Isochronous stress-strain curves were then constructed considering the strain of the specimens at different creep stresses at selected times between 200 and 1000 s.

RESULTS AND DISCUSSIONS

In Figure 2 TEM images of the LLDPE-A380-2 nanocomposite sample at different magnification levels are reported. It is easy to detect the presence of spherical silica aggregates uniformly dispersed in the matrix, with mean diameter of about 200 nm. This means that the relatively high shear forces applied during the melt compounding process led to a satisfactory dispersion of the nanofiller.

The effect of the fumed silica nanofiller on the isothermal tensile creep at different stresses is visualized in Fig. 3. As expected, the creep compliance of LLDPE is perceptibly higher than that of the composites, if $D(t)$ values obtained under identical loads are compared. In Figure 4 isochronous curves are reported, which were obtained by plotting the creep strain against the applied stress for LLDPE, LLDPE-A200-2, and LLDPE-A380-2 at selected creep times. It can be concluded that incorporated nanosilica increases creep stability, especially when the high surface area nanofiller (A380) is used. As an example, the profound decrease in the creep compliance due to the presence of nanoparticles is evidenced by the fact that isochronous curve of LLDPE-A380-2 sample at 1000 s is very similar to that of neat LLDPE at 200 s. Moreover Fig. 4 indicates that the apparent stress-strain linearity limit does not exceed 1% of strain.

The superposition of the nonlinear creep data necessitates the application of the outlined approach based on the fractional free volume rising with the creep strain. For

 DOI 10.1002/pc

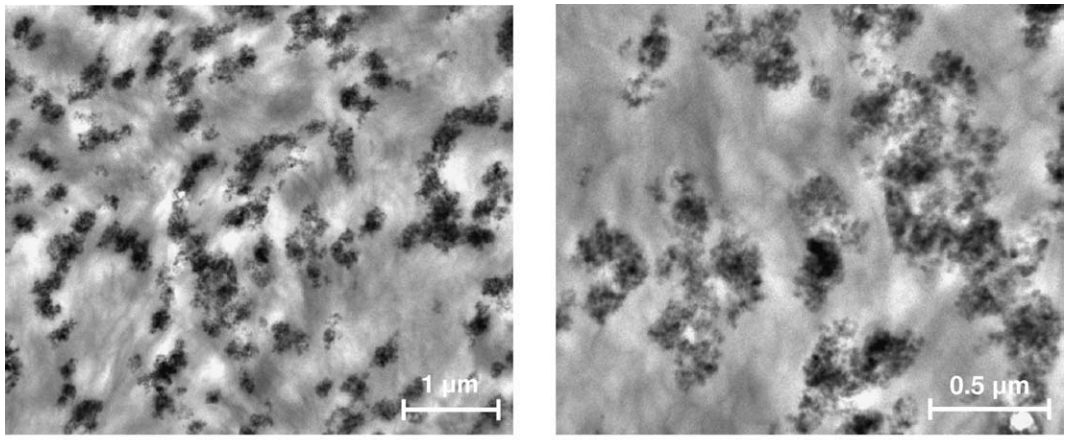

FIG. 2. TEM images of LLDPE-A380-2 sample at different magnifications.

this end, the inputs B, ν, M, f_g, and α_{fv} occurring in *Eqs. 5–11* are required. As no reliable data for LLDPE can be found in existing literature, the aforementioned parameters can only be roughly estimated. As shown in previous articles [39], the ensemble of the parameters making the internal time–strain superposition possible can be varied in some limits. However, it is not possible to arbitrarily anchor the generalized curve on the time scale by manipulating with the inputs, because the superposition is successful only in a "reference state," i.e. in a certain interval on the t^* scale.

The value of B is believed, with regard to its definition, to be a constant close to 1. The determination of Poisson's ratio of thermoplastics and of its possible dependence on strain and/or time is extremely complex and only sporadic data can be found in literature. Usually only a constant value of ν is tabulated to characterize a polymer [22, 23, 42]. As for Poisson's ratio of polyethylene, different experimental values ranging from 0.4 to 0.5 can be found in literature [54–59]. Thus $\nu = 0.44$ reported in articles [57, 59] was chosen for studied LLDPE. The value of $M = 1.51$ was calculated for $\nu_{1cr} = \nu_{2cr} = 0.156$ and $q = 1.8$, by using *Eq. 12*. The fractional free volume in the glassy state and its expansion coefficient are generally taken as universal constants, i.e. $f_g = 0.025$ and $\alpha_{fv} = 0.00048\ K^{-1}$. Adopting these values along with $T_g = -110°C$ [60] for LLDPE, we did not succeed in superposing the creep data. The superposition became viable for $f_g = 0.0125$ and $\alpha_{fv} = 0.0002\ K^{-1}$, which approximately correspond to one half of the universal values. These discrepancies might be attributed to relatively high crystallinity and to the fact that amorphous (noncrystalline) parts are mainly formed loops at the surface of lamellae.

Figure 5 shows that if the creep compliance is plotted against the internal time t^* (calculated by using the indicated inputs), the superposition of the creep curves is quite satisfactory for the neat LLDPE and as well as for the nanocomposites. Generalized curves for the iso-free-volume state given in Fig. 6 indicate that (i) the creep compliance of LLDPE is distinctly higher than that of nanocomposites and (ii) the creep stability of the materials increases with the specific surface area of the nanoparticles. The parameters of *Eq. 10* used for fitting experimental dependencies of neat LLDPE and its nanocomposites are summarized in Table 1. It is evident that this equation is fully satisfactory to fit experimental data of all the tested samples. Table 1 evidences a relatively large scatter of log C^*, probably due to possible irregularities in the read-off displacements shortly after the load imposition. On the other hand, n^* is practically independent of the applied stress in conformity with the concept that n^* is the limiting value for the creep in the pseudo iso-free volume state.

The most practical outcome of the proposed format is that the generalized log $D(t^*)$ vs. log t^* dependence can be utilized for calculating the real log $D(t)$ vs. log t curves for selected stresses. The procedure employs the experimentally found constants log C^* and n^*, which allow us to calculate the compliance $D(t^*)$ for any selected "internal" time t^*. To obtain the corresponding "real" time t we can modify *Eq. 8* by introducing $\varepsilon(t) = \sigma D(t)$

$$\log a_\varepsilon(t) = -\left(\frac{B}{2.303}\right)\frac{\left[(1-2\nu)M\sigma D(t)/\left(f_g+\Delta f_{Tc}\right)\right]}{\left[(1-2\nu)M\sigma D(t)+\left(f_g+\Delta f_{Tc}\right)\right]} \quad (16)$$

and rearrange *Eq. 11*:

$$\log t = \log t^* + \log a_\varepsilon(t) \quad (17)$$

In Figure 7, the log $D(t)$ vs. log t curves for neat LLDPE and for related nanocomposites are calculated and compared with experimental curves. The values of log C^* and n^* used in the calculations were taken from Table 1. As can be seen, the compliance curves predicted for various stresses fit well experimental curves over the considered time interval. Some small discrepancies are evident

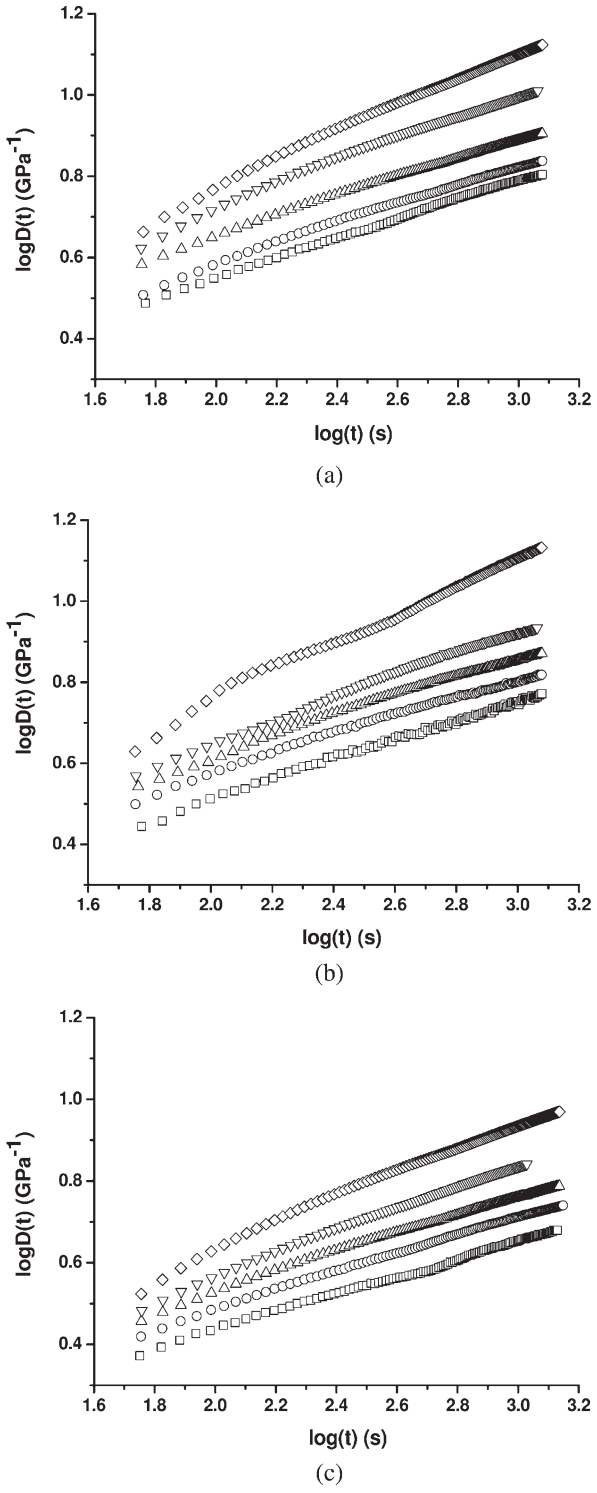

FIG. 3. Creep compliance $D(t)$ of LLDPE and nanocomposites (T = 30°C) as a function of time. (a) LLDPE, (b) LLDPE-A200-2, (c) LLDPE-A380-2. (□) σ_0 = 1 MPa, (○) σ_0 = 2 MPa, (△) σ_0 = 3 MPa, (▽) σ_0 = 4 MPa, (◇) σ_0 = 5 MPa.

only for short times at higher applied stresses, probably because of inaccurate reading of the displacements immediately after the load imposition Fig. 7 clearly demonstrates that the discussed uncertainties in the selection of the inputs B, v, M, f_g, and α_{fv} do not preclude a fairly good prediction of compliance curves. It can be concluded that the applied approach previously developed [3,

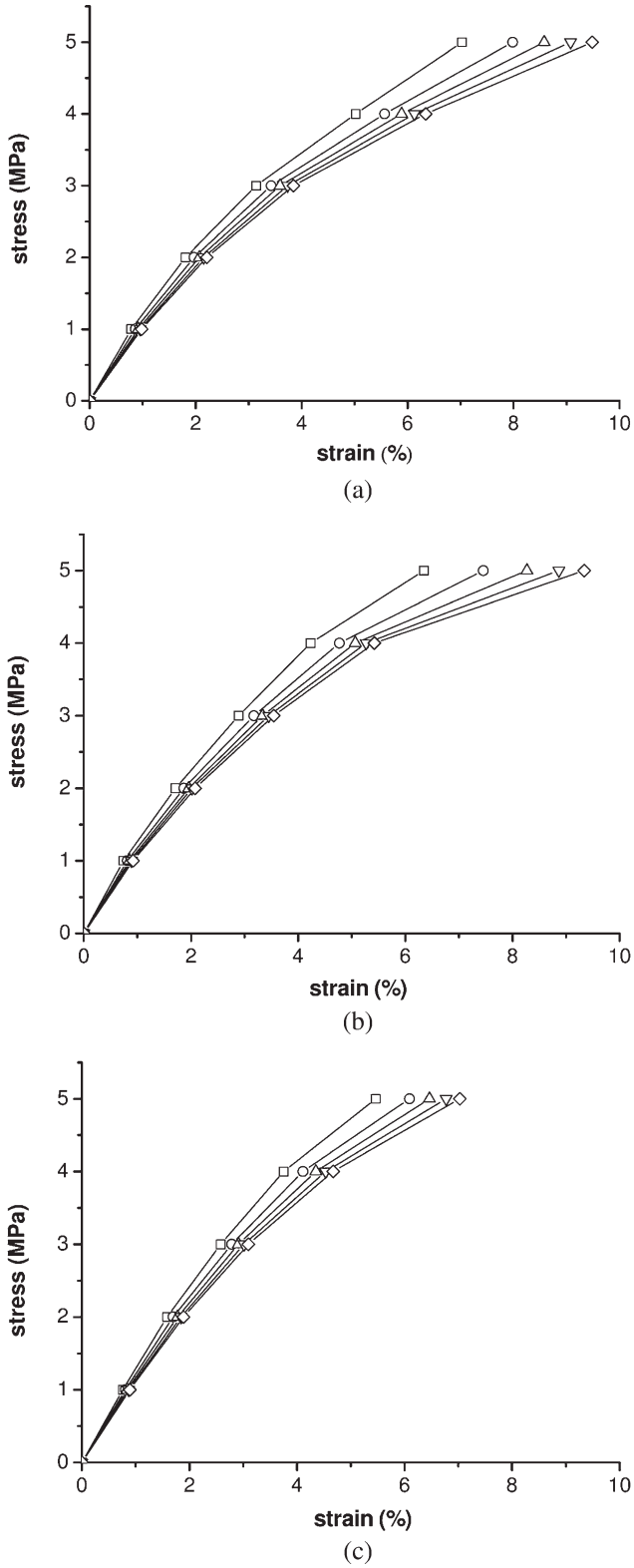

FIG. 4. Isochronous stress–strain curves of LLDPE and nanocomposites (T = 30°C). (a) LLDPE, (b) LLDPE-A200-2, (c) LLDPE-A380-2. (□) t = 200 s, (○) t = 400 s, (△) t = 600 s, (▽) t = 800 s, (◇) t =1000 s.

DOI 10.1002/pc

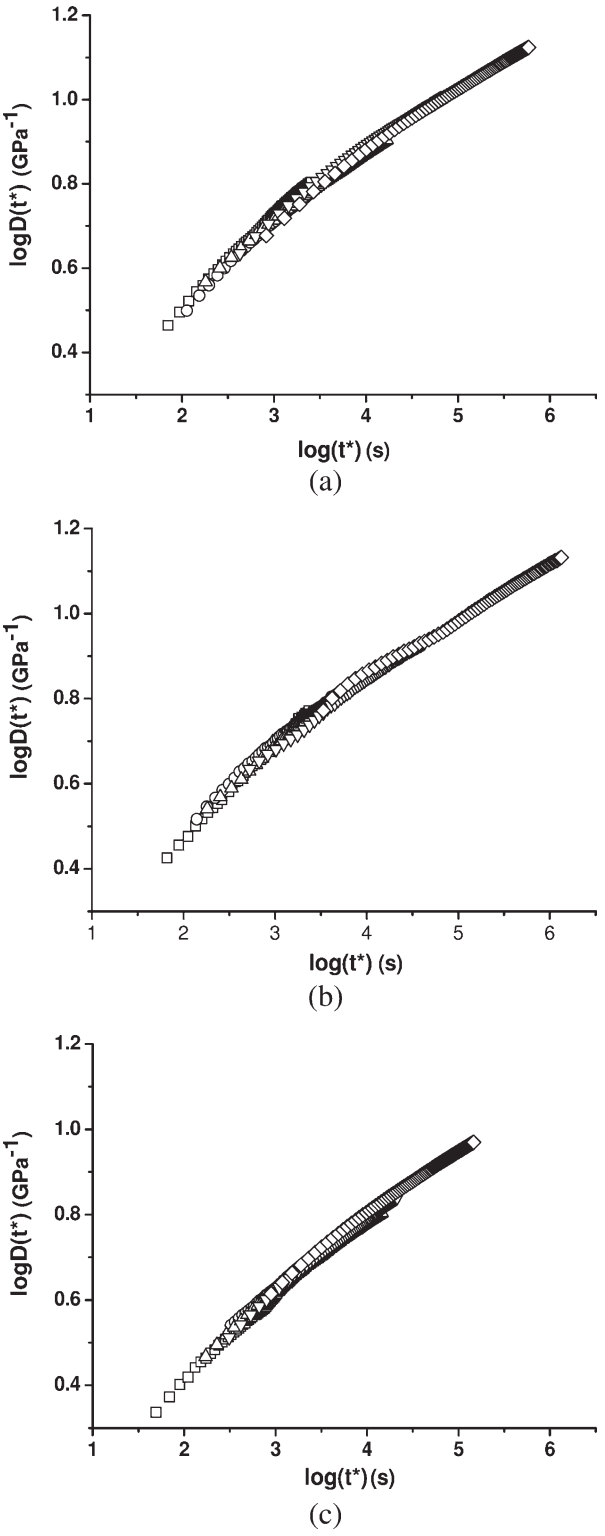

FIG. 5. Superposed creep compliance curves *log* $D(t^*)$ of LLDPE and nanocomposites ($T = 30^\circ$C). (a) LLDPE, (b) LLDPE-A200-2, (c) LLDPE-A380-2. (□) $\sigma_0 = 1$ MPa, (○) $\sigma_0 = 2$ MPa, (△) $\sigma_0 = 3$ MPa, (▽) $\sigma_0 = 4$ MPa, (◇) $\sigma_0 = 5$ MPa.

18, 40] for the nonlinear tensile creep of thermoplastics and their blends can successfully be applied to the LLDPE nanocomposites.

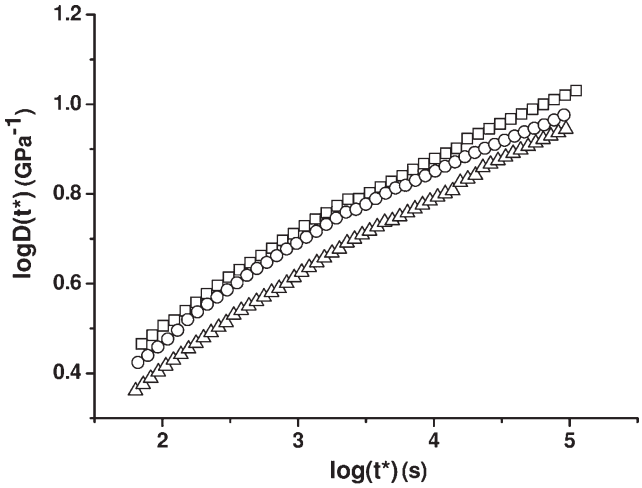

FIG. 6. Generalized curves of the creep compliance *logD*(t^*) of LLDPE and nanocomposites (see *Eqs. 8* and *11*) ($T = 30^\circ$C). (□) LLDPE, (○) LLDPE-A200-2, (△) LLDPE-A380-2.

CONCLUSIONS

Linear low density polyethylene (LLDPE)/fumed silica nanocomposites prepared by melt compounding were used to study the nonlinear viscoelastic creep by means of the previously developed formats for the data processing and the prediction of the nonlinear tensile creep of thermoplastics and their blends. A notable enhancement of the creep resistance with the specific surface area of the nanofillers was found, especially for higher creep stresses. The free volume theory of the viscoelastic creep was for the

TABLE 1. Parameters of *Eq. 10* fitting the creep data of LLDPE and related nanocomposites.

σ_0 (MPa)	*log* C^* [GPa^{-1}]	n^*	R^2
LLDPE			
1	0.0894	0.2117	0.9983
2	0.1509	0.1841	0.9951
3	0.2268	0.1617	0.9963
4	0.2732	0.1523	0.9931
5	0.2954	0.1450	0.9944
Average	0.2071	0.1710	
St.Dev.	0.0860	0.0271	
LLDPE-A200-2			
1	0.0375	0.2183	0.9962
2	0.1337	0.1864	0.9933
3	0.1507	0.1766	0.9950
4	0.2002	0.1604	0.9980
5	0.3310	0.1310	0.9970
Average	0.1706	0.1745	
St.Dev.	0.1073	0.0322	
LLDPE-A380-2			
1	0.0006	0.2050	0.9974
2	0.0935	0.1784	0.9994
3	0.0956	0.1734	0.9952
4	0.0873	0.1765	0.9960
5	0.1676	0.1575	0.9951
Average	0.0889	0.0889	
St.Dev.	0.0593	0.0171	

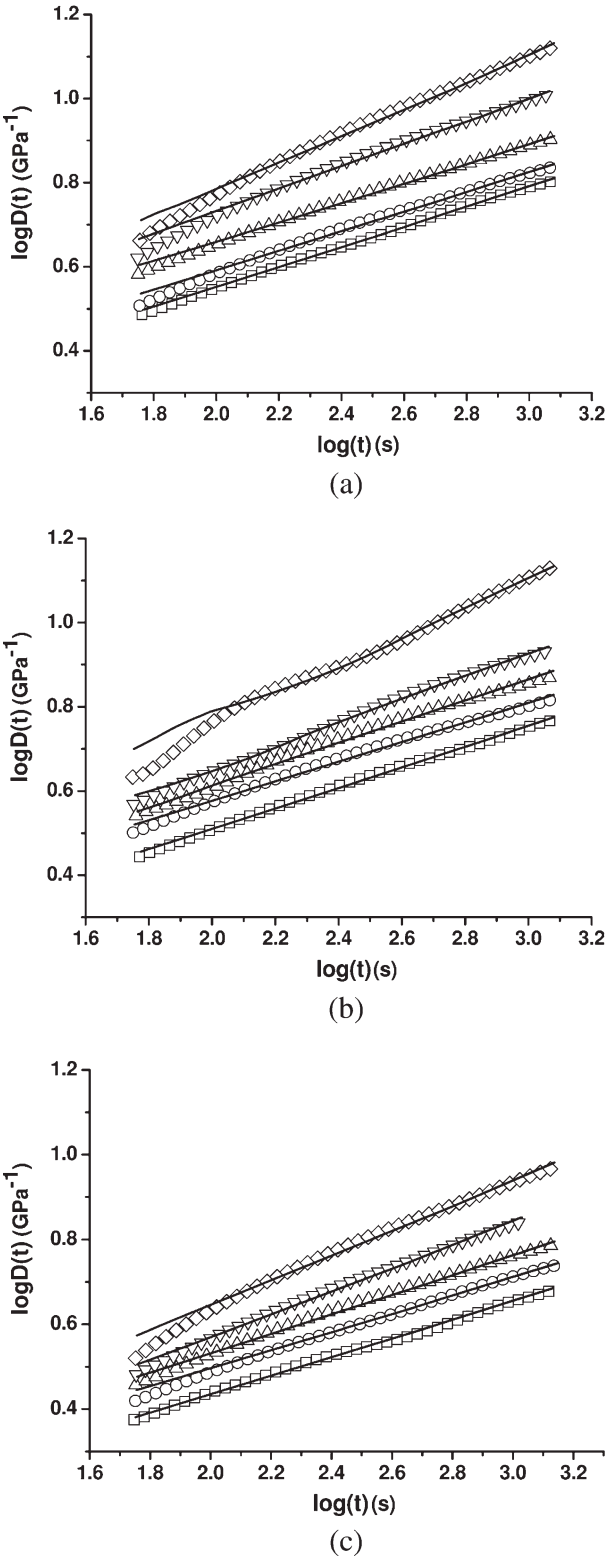

FIG. 7. Creep compliance $D(t)$ of LLDPE and nanocomposites ($T = 30°C$), with the theoretical curves according to *Eq. 10* (solid lines). (a) LLDPE, (b) LLDPE-A200-2, (c) LLDPE-A380-2. (□) $\sigma_0 = 1$ MPa, (○) $\sigma_0 = 2$ MPa, (△) $\sigma_0 = 3$ MPa, (▽) $\sigma_0 = 4$ MPa, (◇) $\sigma_0 = 5$ MPa.

first time successfully used to construct the generalized creep curves of nanocomposites by applying the tensile compliance vs. internal time superposition in the region of nonlinear viscoelasticity. Assuming that the nonlinearity is mainly caused by the strain-induced increment of the free volume, the strain-dependent shift factors were calculated a priori point by point to superpose compliance curves detected at various stresses. The proposed superposition procedure was found viable for both neat LLDPE and nanocomposites with different nanosilicas. A most practical outcome consists in that the generalized compliance dependences constructed for the pseudo iso-free volume state of a material can be employed for predicting the real time-dependent compliance for any selected stress in the region of fully reversible deformations.

REFERENCES

1. F. Hussain, M. Hojjati, M. Okamoto, and R.E. Gorga, *J. Compos. Mater*., **40**, 1511 (2006).
2. J. Kolarik, L. Fambri, A. Pegoretti, and P. Goberti, *Polym. Eng. Sci*., **161**, 42 (2002).
3. J. Kolarik, A. Pegoretti, L. Fambri, and A. Penati, *J. Appl. Polym. Sci*., **641**, 88 (2003).
4. A. Pegoretti, *Nano- and Micromechanics of Polymer Blends and Composites*, Hanser, Munich (to appear).
5. O. Starkova, J. Yang, and Z. Zhang, *Comp. Sci. Tech*., **67**, 2691 (2007).
6. J.L. Yang, Z. Zhang, A.K. Schlarb, and A.K. Schlarb, *Polymer*, **47**, 2791 (2006).
7. Z. Zhang, J.L. Yang, and K. Friedrich, *Polymer*, **45**, 3481 (2004).
8. S. Siengchin, J. Karger-Kocsis, and R. Thomann, *J. Appl. Polym. Sci*., **105**, 2963 (2007).
9. A. Ranade, K. Nayak, D. Fairbrother, and N.A. D'Souza, *Polymer*, **46**, 7323 (2005).
10. F. Bondioli, A. Dorigato, P. Fabbri, M. Messori, and A. Pegoretti, *Polym. Eng. Sci*., **48**, 448 (2008).
11. F. Bondioli, A. Dorigato, P. Fabbri, M. Messori, and A. Pegoretti, *J. Appl. Polym. Sci*., **112**, 1045 (2009).
12. A. Pegoretti, A. Dorigato, and A. Penati, *Express Polym. Lett*., **1**, 123 (2007).
13. Z.D. Wang and X.X. Zhao, *Mater. Sci. Eng. A*., **486**, 517 (2008).
14. A. Pegoretti, M.L. Accorsi, and A.T. Dibenedetto, *J. Mater. Sci*., **6145**, 31 (1996).
15. S.K. Friedlander, *Smoke, Dust and Haze: Fundamental of Aerosol Behavior*, Wiley, New York (1977).
16. E. Kontou and M. Niaounakis, *Polymer*, **47**, 1267 (2006).
17. W. Andrew, *The Effect of Creep and Other Time Related Factors on Plastics and Elastomers*, Plastics Design Library, New York (1991).
18. J. Kolarik, *J. Pol. Sci. Part B: Pol. Phys*., **41**, 736 (2003).
19. F. Bueche, *Physical Properties of Polymers*, Interscience, New York (1962).
20. J.D. Ferry, *Viscoelastic Properties of Polymers*, Wiley, New York (1980).
21. R.S. Lakes, *Viscoelastic Solids*, CRC Press, London (1999).
22. D.R. Moore and S. Turner, *Mechanical Evaluation Strategies for Plastics*, Woodhead, Cambridge (2001).

 DOI 10.1002/pc

23. L.E. Nielsen and R.F. Landel, *Mechanical Properties of Polymers and Composites*, Dekker, New York (1994).
24. E. Riande, *Polymer Viscoelasticity, Stress and strain in Practice*, Dekker, New York (2000).
25. F. Rodriguez, *Principles of Polymer Systems*, Taylor & Francis, Washington DC (1996).
26. I.M. Ward and D.W. Hadley, *An Introduction to the Mechanical Properties of Solid Polymers*, Wiley, Chichester (1993).
27. D.M. Colucci, P.A. O'Connell, and G.B. McKenna, *Polym. Eng. Sci.*, **37**, 1469 (1997).
28. W.G. Knauss and I. Emri, *Polym. Eng. Sci.*, **27**, 86 (1987).
29. H. Lu, X. Zhang, and W.G. Knauss, *Polym. Compos.*, **18**, 211 (1997).
30. C.F. Popelar and K.M. Liechti, *Mech. Time-Depend. Mater.*, **7**, 89 (2003).
31. S. Turner, *Polym. Eng. Sci.*, **6**, 306 (1966).
32. G.U. Losi and W.G. Knauss, *Polym. Eng. Sci.*, **32**, 542 (1992).
33. P.A. O'connell and G.B. McKenna, *Polym. Eng. Sci.*, **37**, 1485 (1997).
34. C.F. Popelar and K.M. Liechti, *J. Eng. Mater. Tech.*, **119**, 205 (1997).
35. J. Lai and A. Bakker, *Polymer*, **36**, 93 (1995).
36. J.D. Ferry, R.A. Stratton, and Z. Koll, **171**, 107 (1960).
37. S. Goyanes, W. Salguerio, A. Somoza, J.A. Ramos, and I. Mondragon, *Polymer*, **45**, 6691 (2004).
38. D. Kilburn, D. Bamford, G. Dlubek, J. Pionteck, and M.A. Alam, *J. Pol. Sci. B: Pol. Phys.*, **41**, 3089 (2003).
39. J. Kolarik and A. Pegoretti, *Polymer*, **47**, 346 (2006).
40. J. Kolarik, A. Pegoretti, L. Fambri, and A. Penati, *Macromol. Mater. Eng.*, **288**, 629 (2003).
41. J. Kolarik, A. Pegoretti, L. Fambri, and A. Penati, *Polym. Eng. Sci.*, **46**, 1363 (2006).
42. R.J. Crawford, *Plastics Engineering*, Butterworth-Heinemann, Oxford, (1988).
43. M. Schlimmer, *Rheol. Acta.*, **18**, 62 (1979).
44. P.E. Tomlins, *Polymer*, **37**, 3907 (1996).
45. R.W. Garbella, J. Wachter, and J.H. Wendorf, *Prog. Colloid. Polym. Sci.*, **71**, 164 (1985).
46. N.G. McCrum, B.E. Read, and G. Williams, *Anelastic and dielectric Effects in Polymeric solids*, Dover, New York (1984).
47. J. Kolarik, *Polym. Eng. Sci.*, **36**, 2518 (1996).
48. J. Kolarik, *Eur. Polym. J.*, **34**, 585 (1998).
49. J. Kolarik, *J. Macromol. Sci. Phys.*, **B39**, 53 (2000).
50. J. Kolarik, L. Fambri, A. Pegoretti, and A. Penati, *Polym. Eng. Sci.*, **40**, 127 (2000).
51. P.G. De Gennes, *J. Phys. Lett.*, **37**, L1 (1976).
52. W.Y. Hsu and S. Wu, *Polym. Eng. Sci.*, **33**, 293 (1993).
53. J. Sax and J.M. Ottino, *Polym. Eng. Sci.*, **23**, 165 (1983).
54. D.I. Bower, *An introduction to Polymer Physics*, Cambridge University Press, Cambridge (2002).
55. S. Fakirov and D. Bhattacharyya, *Handbook of Engineering Biopolymers: Homopolymers, Blends and Composites*, Hanser, Germany (2007).
56. S.M. Kurtz, *UHMWPE Biomaterials Handbook: Ultra High Molecular Weight Polyethylene in Total Joint Replacement and Medical Devices*, Academic Press, China (2009).
57. M. Meyyappan, *Carbon Nanotubes: Science and Appllications*, CRC Press, USA (2005).
58. D. Shi, *Introduction Biomaterials*, World Scientific Publishing, USA (2006)
59. C. Wei, D. Srivastava, and K. Cho, *Nano. Lett.*, **2**, 647 (2002).
60. W. Martienssen and H. Warlimont, *Springer Handbook of Condensed Matter and Materials Data*, Springer, Berlin, (2005).